ACS OMEGA

Open Access

http://pubs.acs.org/journal/acsodf

Article

Crosstalk between Aldosterone and Glycation through Rac-1 Induces Diabetic Nephropathy

Mayura Apte, Mohd Shahnawaz Khan, Nilima Bangar, Armaan Gvalani, Huma Naz, and Rashmi S. Tupe*

Cite This: *ACS Omega* 2023, 8, 37264−37273

Read Online

ACCESS | Metrics & More | Article Recommendations | Supporting Information

ABSTRACT: **Background:** Advanced glycation end products (AGEs) interaction with its receptor (RAGE) and aldosterone (Aldo) through the mineralocorticoid receptor (MR) activates Rac-1 and NF-κB independently in diabetic nephropathy (DN). However, the crosstalk of Aldo with AGEs-RAGE is still unresolved. Our study examined the impact of the AGEs-Aldo complex on renal cells and its effect on the RAGE-MR interaction. **Methods and results:** Glycation of human serum albumin (HSA) (40 mg/mL) with methylglyoxal (10 mM) in the presence of Aldo (100 nM) and aminoguanidine (AG) (100 nM) was performed. Glycation markers such as fructosamine and carbonyl groups and fluorescence of AGEs, pentosidine, and tryptophan followed by protein modification were measured. Renal (HEK-293T) cells were treated with the glycated HSA-Aldo (200 μg/mL) along with FPS-ZM1 and spironolactone antagonists for RAGE and Aldo, respectively, for 24 h. Glycation markers and esRAGE levels were measured. Protein and mRNA levels of RAGE, MR, Rac-1, and NF-κB were estimated. Glycation markers were enhanced with Aldo when albumin was only 14−16% glycated. AGEs-Aldo complex upregulated RAGE, MR, Rac-1 and NF-κB expressions. However, FPS-ZM1 action might have activated the RAGE-independent pathway, further elevating MR, Rac-1, and NF-κB levels. **Conclusion:** Our study concluded that the presence of Aldo has a significant impact on glycation. In the presence of AGEs-Aldo, RAGE-MR crosstalk exerts inflammatory responses through Rac-1 in DN. Insights into this molecular interplay are crucial for developing novel therapeutic strategies to alleviate DN in the future.

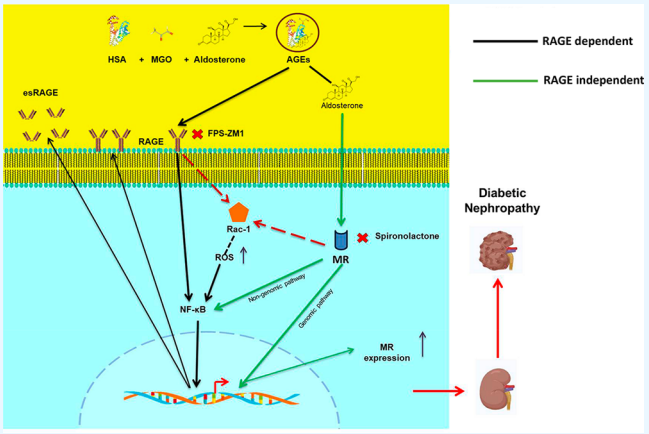

1. INTRODUCTION

Diabetic nephropathy (DN) is one of the many causes of end-stage renal disease,[1] and hyperglycemia plays a significant role in its progression. It is documented that during hyperglycemia the secretion of Aldosterone (Aldo), a mineralocorticoid, increases through the renin-angiotensin system. Aldo has a principal role in maintaining electrolyte and fluid homeostasis. Binding of Aldo to mineralocorticoid receptor (MR) activates genomic or nongenomic signaling pathways in distal renal tubule cells.[2,3] Downstream effects of nongenomic pathways, such as reactive oxygen species (ROS) generation and inflammation induction, can be MR-dependent or MR-independent.[4] Earlier, it was found that Aldo-MR activation in the presence of Ras-related C3 botulinum toxin substrate (Rac-1) has a significant role in the pathogenesis of renal damage.[5] The activated Rac-1 was found to regulate NF-κB and its translocation to the nucleus, further inducing expression of pro-inflammatory cytokines.[6]

Additionally, hyperglycemia disturbs metabolic pathways, most of which are associated with increased levels of AGEs. The nonenzymatic glycation reaction between free amino groups of proteins and reactive carbonyl groups of reducing sugars leads to the formation of AGEs.[7] Interaction of AGEs with Receptor of Advanced Glycation end products (RAGE) activates various downstream signaling pathways,[8] inducing inflammation, insulin resistance, and aging.[9] The AGEs-RAGE interaction was also reported to stimulate Rac-1, activating nuclear factor-κB (NF-κB) further leading to inflammation.[10] Moreover, AGEs accumulation-induced podocyte injury, renal tubular epithelial injury, and urinary albumin excretion were reduced in diabetic rats when treated with RAGE antagonist − N-Benzyl-4-chloro-N-cyclohexylbenzamide (FPS-ZM1).[11] This reduced the damaging effect of AGEs-RAGE activation in DN.

Received: July 15, 2023
Accepted: September 14, 2023
Published: September 28, 2023

In addition to full-length RAGE, there are circulating soluble RAGE isoforms without a trans-membrane domain and cytoplasmic tail, namely, soluble RAGE (sRAGE), endogenously secretory form (esRAGE), and cleaved form (cRAGE).[12] esRAGE arises by alternative splicing of full-length RAGE (FL-RAGE) gene *AGER (advanced glycation end product receptor)*. cRAGE arises by proteolytic cleavage of RAGE by a disintegrin, ADAM10, and membrane Type-1 Matrix metalloproteinases.[13] Both of these function as decoy receptors, prevent interaction of AGEs with FL-RAGE, and attenuate signal transduction pathways, reducing inflammation and oxidative stress.[12,13]

It was found that Aldo raises carboxymethyl lysine (CML), one of the AGEs, and promotes the positive feedback loop by RAGE leading to downstream signaling, while CML enhances MR expression indicating correlation between RAGE and MR.[2] MR antagonist, spironolactone, was observed to downregulate RAGE expression.[14] However, the crucial interaction between AGEs-RAGE and Aldo-MR through Rac-1 remains to be discovered. Aldo can have this interaction as a RAGE-dependent or independent mechanism. Our earlier study reported static and spontaneous interaction between Aldo and glycated HSA.[15] Thus, this study emphasizes evaluating the Aldo effect on glycation modifications of albumin and RAGE expression in HEK-293T cells. Glycation markers (fructosamine content, carbonyl groups, pentosidine, AGEs, and tryptophan fluorescence) and protein modifications (HPLC, phenyl boronate affinity chromatography) were estimated in glycated HSA samples with or without Aldo. Moreover, the molecular MR-Rac-1-RAGE axis in renal cells in the presence of Aldo during glycation was studied by analyzing expressions of RAGE, MR, Rac-1, and NF-κB using the HEK-293T cell line.

2. MATERIALS AND METHODS

2.1. Materials. HSA (A1653), methylglyoxal (MGO), aminoguanidine (AG), and Aldo were procured from Sigma-Aldrich (St. Louis, United States). Reagents required for glycation marker assays − Folin-Ciocalteau reagent, nitroblue tetrazolium (NBT), dinitrophenylhydrazine (DNPH), and trichloroacetic acid were acquired from SRL (Mumbai, India) and HiMedia (Mumbai, India). The materials required for cell culture work − DMEM, FBS, and 1% antibiotic/antimycotic solution were obtained from Gibco (Waltham, United States) and HiMedia (Mumbai, India). Primary antibodies for CML (MAB3247), RAGE (MAB11451), NF-κB (SC8008), β-actin (SC130301), and secondary antibody HRP conjugated goat antimouse IgG were procured from R&D systems (Minneapolis, United States) and Santacruz (Dallas, United States). SYBR green was obtained from Applied Biosystems (Waltham, United States). Primers for RT-qPCR were acquired from Bioserve Biotechnologies (Hyderabad, India).

2.2. In Vitro Glycation of HSA. In vitro glycation of HSA at a concentration of 40 mg/mL was performed in phosphate buffer saline (PBS) using the previously reported method[16] with slight modifications. HSA was glycated with 10 mM methylglyoxal (MGO) prepared in PBS for 48 h at 37 °C in the presence of aminoguanidine (AG) (standard glycation inhibitor) (100 nM)[15] and Aldo (100 nM),[17] separately. Native HSA, glycated HSA, i.e., HSA + MGO (G.HSA), G.HSA + Aldo, and G.HSA + AG were sustained under sterile conditions. Samples were then subjected to extensive dialysis for 48 h at 4 °C with 3 PBS changes a day and were filtered using 0.22 μm syringe filters and stored at −20 °C in sterile cryovials. Protein concentrations of each sample were estimated using the Folin-Lowry method[18] before further analysis.

2.3. Estimation of Glycation Markers in the Presence of Aldo. *2.3.1. Fructosamine Content.* Fructosamine content was estimated as per the described method[19] with slight modifications. Nitroblue tetrazolium (0.75 mM) was added to HSA and G.HSA samples followed by the addition of 1 M NaOH. Reaction mixtures were incubated at 37 °C for 30 min. Absorbance was measured at 530 nm on an Eon Biotek plate reader, Synergy H1 (Agilent, Santa Clara, United States). 1-Deoxy-1-morpholino-D-fructose was used as a primary standard to calculate the fructosamine content expressed in nM of fructosamine/mg protein.

2.3.2. Carbonyl Content. Dinitrophenylhydrazine (10 mM) dissolved in 2.5 M HCl was added to previously glycated HSA samples and then incubated at RT for 1 h. After incubation, 20% trichloroacetic acid was added to reaction mixtures and centrifuged for 10 min at 15,000 *g*. The obtained pellet was washed with ethyl acetate: ethanol (1:1) by centrifugation at 7669 *g* for 10 min. Urea (6 M) was used to solubilize the pellet, and then absorbance was taken at 365 nm on an Eon Biotek plate reader, Synergy H1 (Agilent, Santa Clara, United States). The protein carbonyl content was analyzed using the reported method.[20]

2.3.3. Fluorescence of Tryptophan, AGEs, and Pentosidine. AGEs and pentosidine formation were analyzed by measuring the fluorescence of samples at excitation wavelengths of 370 and 335 nm and emission wavelengths of 440 and 400 nm, respectively. Tryptophan fluorescence was measured at an excitation wavelength of 280 nm and an emission wavelength of 360 nm.[21] The fluorescence was measured on an Eon Biotek plate reader, Syngery H1 (Agilent, Santa Clara, United States).

2.3.4. Estimation of CML by Western Blotting. Western blotting was performed as per the previously described method.[22] SDS-Polyacrylamide gel was prepared (12% resolving and 5% stacking gel). 40 μg portion of HSA and glycated HSA samples were mixed with loading dye. The sample mixture was heated at 95 °C for 5 min. Then equal volumes of the above sample mixtures were loaded in the gel. The gel was run at 70 V and then placed on a nitrocellulose membrane for protein transfer on ice. Protein transfer was done at 95 V for 90 min. Three washes of TBST (10 min each) (Tris Buffered Saline +1% Tween 20) (1X) were given to the membrane and then 5% BSA was used for blocking at 4 °C overnight. The membrane was then incubated with primary antibody of CML (1 μg/mL in 5% BSA) overnight at 4 °C. Afterward, the secondary antibody treatment (1:1000 in 3% BSA) of HRP conjugated goat antimouse IgG was given to the membrane at RT for 1 h. Three washes of TBST are followed by visualization using the enhanced chemiluminescence kit (1705060) on SYNGENE G: BOX (Cambridge, United Kingdom).

2.3.5. HPLC Analysis. To determine the formation of the AGEs adduct in the presence of Aldo and AG, HPLC analysis of the above-glycated samples was performed according to a previously reported method[22] with slight modifications. It was performed on a Shimadzu prominence liquid chromatography (Shimadzu Kyoto, Japan) system incorporated with a UV/visible detector using a C18 column. Eluents A (0.1% trifluoroacetic acid and 5% acetonitrile) and B (0.1% trifluoroacetic acid and 95% acetonitrile) were used to maintain an isocratic condition of 60% B up to 10 min at a constant flow rate. The chromatogram was measured at 264 nm at 40 °C by loading 20 μL of samples (100 μg/mL).

https://doi.org/10.1021/acsomega.3c05085
ACS Omega 2023, 8, 37264−37273

2.3.6. Phenyl Boronate Affinity Chromatography. Phenyl boronate affinity chromatography was used to determine the extent of glycation in the presence of Aldo with slight modifications.[23] Affinity chromatography column (2 × 1 cm) was packed with m-aminophenylboronic acid agarose and subjected to equilibration with 50 mM potassium phosphate buffer (pH 7.8) containing 1 M NaCl for 24 h. After equilibration, the column was rinsed with a potassium phosphate buffer. One mL of 100 μg/mL HSA sample was subjected to the column. Unbound fractions were eluted using elution buffer A (50 mM Taurine, pH 8.7 adjusted with NaOH + 200 mM $MgCl_2$) to wash off nonglycated proteins. Elution buffer B (50 mM Taurine, pH 8.7 adjusted with NaOH + 50 mM tris HCl) was used to wash out bound glycated proteins, and absorbance was measured at 280 nm on an Eon Biotek plate reader (Agilent, Santa Clara, United States).

2.4. HEK-293T Cell Treatment with Glycated HSA and Aldo. *2.4.1. Cell Maintenance and Treatment.* HEK-293T cells were acquired from the National Centre for Cell Science, Pune, and maintained in DMEM supplemented with 10% Fetal Bovine Serum + 1% antibiotic/antimycotic solution. The confluent flasks were split into 1:3 ratios and were used for the treatment with previously glycated HSA + Aldo (200 μg/mL) samples along with spironolactone and FPS-ZM1, 100 nM each. The treatment duration was 24 h at 37 °C, and images were taken under 40X at 0 and 24 h. Cell lysates were then prepared using RIPA buffer (1% protease inhibitor and 10% phosphatase inhibitor) and further used to analyze the glycation markers and for Western blotting and RT-qPCR.

2.4.2. Cellular Glycation Markers. Glycation markers of cells such as fructosamine content, carbonyl groups, AGEs, pentosidine, and tryptophan fluorescence were analyzed as described previously in Section 2.3.

2.4.3. esRAGE Estimation by ELISA. Quantification of esRAGE from the cell culture supernatant was carried out using the ELISA kit (IT3856), G-Biosciences. According to the manufacturer's instructions, 0.1 mL of diluted supernatant was added to each well and kept at 37 °C for 90 min. Biotinylated Detection Antibody working solution (100 μL) was added into the above mixture and kept for 1 h. Addition of working solution of ELISA Detection Reagent (100 μL) was followed by 30 min of incubation at 37 °C. The plate was washed five times and incubated with 90 μL of ELISA Detection Substrate (TMB) at the same conditions as mentioned earlier. Further, 50 μL of stop solution was used to stop the reaction. Absorbance at 450 nm was recorded immediately on an Eon Biotek plate reader, Syngery H1(Agilent, Santa Clara, United States).

2.4.4. Intracellular ROS Detection using DCF-DA. In a 35 mm Petri dish, approximately 10^6 cells were seeded with a coverslip and maintained in DMEM. Cells were treated with previously glycated samples for 24 h. A wash of 1X PBS was given to cells followed by DCF-DA (20 μM) staining for 30 min at 37 °C. The excess stain was removed by giving a wash with 1X PBS. The coverslip was mounted with the help of 90% glycerol. Imaging was performed using a green fluorescent protein filter on a fluorescence microscope, EVOS M5000 (Invitrogen, Waltham, United States).[22]

2.4.5. Western Blotting. To understand the expressions of RAGE and NF-κB, Western blotting of cell lysates (30 μg) of different treatment groups was performed as per the previously mentioned method in section 2.3.4. The membrane was then incubated overnight with primary antibodies of RAGE (1 μg/mL in 5% BSA) or NF-κB (1:1000 in 5% BSA) or β-actin (1:1000 in 5% BSA) at 4 °C. After three washes of TBST (Tris Buffered Saline +1% Tween 20) (1X), the membrane was developed at RT with a secondary antibody solution (1:1000 ratios in 3% BSA) of HRP-conjugated goat antimouse IgG 1 h. Proteins were then visualized on a SYNGENE G: BOX (Cambridge, United Kingdom) using the enhanced chemiluminescence (ECL) kit[22] followed by densitometry analysis with the help of the ImageJ 1.44p gel analysis tool.

2.4.6. RT-qPCR. Total RNA isolation from cells of different treatment groups was carried out using TRIzol reagent, and cDNA was synthesized using the iScript c-DNA synthesis kit (1708891). RT-qPCR was accomplished in a BioRad CFX-96 system (Hercules, United States). The cDNA was amplified using primers reported in Table 1 and SYBR green PCR master mix to analyze RAGE, NF-κB, MR, and Rac-1 expressions. The relative quantity of the target gene against internal control (β-actin) was expressed as $2^{-\Delta\Delta Ct}$.[2]

Table 1. Primer Sequences Used for the RT-qPCR Gene Primer Reference[a]

gene	primers	reference
RAGE	F: 5′CTACCGAGTCCGTGTCTACCA3′	46
	R: 5′CATCCAAGTGCCAGCTAAGAG3′	
NF-κB	F: 5′GCTTAGGAGGGAGAGCCCA3′	47
	R: 5′GGTATGGGCCATCTGCTGTT3′	
MR	F: 5′GAGAAAAGCCCGTCTGTTTG3′	48
	R: 5′AGAGGAGTTCCCTGGGTGAT3′	
Rac-1	F: 5′AGGACACGATTGAGAAGCTGAAGG3′	49
	R: 5′CACTGTCTTGAGTCCTCGCTGTG3′	
β-actin	F: 5′GATGCAGAAGGAGATCACTGC3′	50
	R: 5′ATACTCCTGCTTGCTGATCCA3′	

[a]F: Forward primer, R: Reverse primer.

2.5. Statistical Analysis. Statistical analysis was performed using Graph Pad Prism software (version 8.01). One-way analysis of variance (ANOVA) coupled with Tukey analysis was carried out to compare the difference between the mean of different samples. p-value <0.05 was considered significant. Data are represented as mean ± SD of experiments performed in triplicate.

3. RESULTS

3.1. Effect of Aldo on Albumin Glycation Markers. To determine the glycation modifications, various glycation markers were measured. As depicted in Figure 1, glycation markers such as fructosamine content, AGEs, and pentosidine fluorescence were considerably higher in G.HSA + Aldo ($p < 0.0001$) as compared to HSA (Figure 1a−c). Carbonyl group content was increased in G.HSA in comparison to that of G.HSA + Aldo (fold change = 1.40) (Figure 1e). Reduction in tryptophan fluorescence (Figure 1d), in G.HSA + Aldo (1.88 folds, $p < 0.0001$), indicated glycation-induced structural changes when compared to HSA. There was no significant difference observed between samples having AG and G.HSA. However, in the presence of AG, the carbonyl group content was observed to be low (1.72 folds, $p < 0.01$).

As observed from Figure 1f, glycation aggregate bands above prominent HSA are specifically dominated by CML adducts. The densitometry analyses of the aggregates indicate significant CML adducts in all glycated samples (Figure 1g). Aggregate formation was higher in G.HSA compared to G.HSA + Aldo, whereas G.HSA + AG did not inhibit aggregate formation.

https://doi.org/10.1021/acsomega.3c05085
ACS Omega 2023, 8, 37264−37273

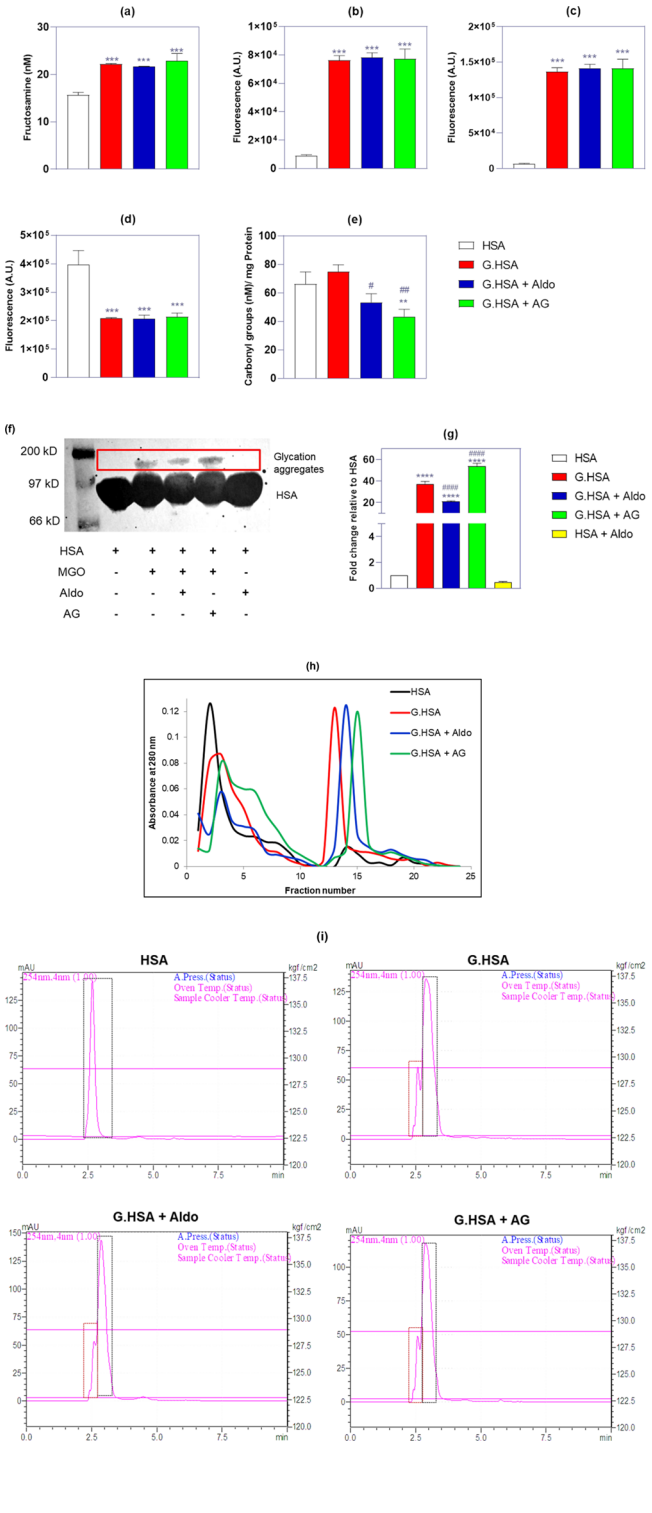

Figure 1. Glycation modifications at intermediate levels. HSA (40 mg/mL) was glycated with MGO (10 mM) along with Aldo (100 nM) for 48 h at 37 °C and after dialysis glycated samples were further subjected to analyze different glycation markers − (a) fructosamine content; (b) AGEs fluorescence; (c) pentosidine fluorescence; (d) tryptophan fluorescence; (e) carbonyl groups; readings were calculated per mg of protein; (f) CML formation; (g) densitometry analysis of CML formation; (h) extent of glycation evaluated by phenyl boronate affinity chromatography; (i) elution profile of glycated samples with Aldo and AG. The data is presented as mean ± SD, $n = 3$, *$p < 0.05$, **$p < 0.01$, ***$p < 0.001$, *indicates p value in comparison to HSA; $^{\#\#}p < 0.1$, $^{\#\#\#}p < 0.01$, $^{\#}$indicates p value in comparison to G.HSA.

The degree of glycation in treated albumin samples was evaluated by phenyl boronate affinity chromatography (Figure 1h). As expected, HSA was eluted in earlier fractions with elution buffer A. However, the amount of modified protein eluted with elution buffer B is much more in G.HSA and G.HSA + Aldo or AG. This indicated the existence of an altered albumin structure.

To get more insight into glycation-induced modifications, HPLC was performed (Figure 1i). The elution profile of G.HSA + Aldo showed induced conformational changes. HSA elution profile displayed one single peak at a retention time of 2.66 min, covering 95.59% area. However, the G.HSA elution profile yielded two different peaks indicating the formation of AGEs adduct at a retention time of 2.57 min covering 14% area. The shift in the area of HSA was observed at a retention time of 2.85 min. The presence of Aldo also yielded two different peaks. AGEs adduct formation was observed at the same retention time as that of G.HSA, covering a 12% area. The elution profile in the presence of AG showed AGEs adduct formation at a retention time of 2.57 min covering 14.18% area. In all three glycated HSA samples, a shift in the area of HSA was observed, indicating the formation of AGEs. Almost 80% of HSA remains unmodified (Table 2).

Table 2. Concentration of Unmodified and Modified HSA in the Presence of Aldosterone and AG

sample	unmodified albumin (% area)	modified albumin (% area)
HSA	95.59	4.41
G.HSA	85.09	14.91
G.HSA + Aldo	83.64	16.36
G.HSA + AG	84.77	15.23

3.2. Aldo Influence on Cellular Glycation Modifications. Renal cell exposure to G.HSA + Aldo enhanced glycation modifications compared to that of G.HSA only. Fructosamine formation in G.HSA + Aldo treatment increased by 1.11-fold ($p < 0.01$) (Figure 2a). Higher AGEs and pentosidine fluorescence were observed in G.HSA + Aldo (1.44 folds, $p < 0.001$) compared to HSA (Figure 2b,c). Nonetheless, FPS-ZM1 (1.61 folds, $p < 0.001$) and spironolactone (1.10 folds, $p < 0.001$) presence reduced glycation independently in terms of reduced AGEs and pentosidine fluorescence. However, higher fluorescence after administration of both antagonists might be because of the activation of an alternative pathway. The treatment of G.HSA and G.HSA + Aldo resulted in considerably low tryptophan fluorescence, whereas the same was restored with the addition of both antagonists (Figure 2d). Cellular morphology and viability were found to be affected by the presence of G.HSA and Aldo (Figures S1 and S2).

3.3. Aldo Effect on the Cellular Protein Expressions of RAGE and NF-κB. The AGEs-RAGE interaction initiates signaling cascade and activates NF-κB causing inflammation. The treatment of G.HSA elevated protein expressions of RAGE ($p < 0.0001$) and NF-κB ($p < 0.01$) compared to HSA treatment (Figure 3a−c). Though G.HSA + Aldo did not show any effect on RAGE expression, interestingly, HSA + Aldo treatment amplified RAGE protein expression significantly. RAGE expression was reduced with the treatment of spironolactone ($p < 0.0001$), FPS-ZM1 ($p < 0.0001$) and the combination of both ($p < 0.0001$) (Figure 3b). This suggests that Aldo-MR pathway-dependent activation of RAGE. G.HSA + Aldo

https://doi.org/10.1021/acsomega.3c05085
ACS Omega 2023, 8, 37264−37273

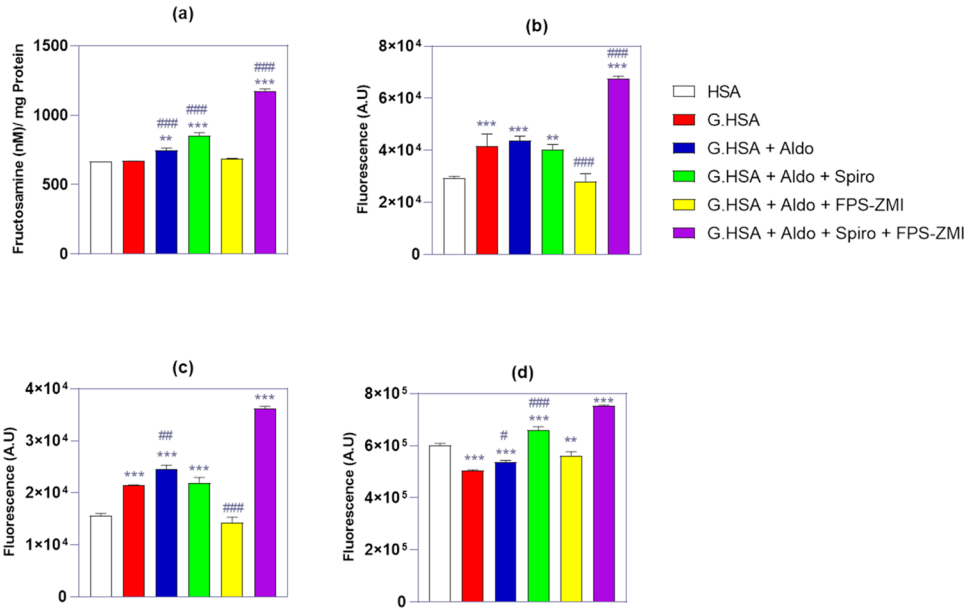

Figure 2. Effect of Aldo on cellular glycation modifications. HEK293T cells were treated with 200 μg/mL of glycated samples for 24 h. Cells were then lysed and lysate was further used to analyze glycation markers − (a) fructosamine content, (b) AGEs fluorescence; (c) pentosidine fluorescence; (d) tryptophan fluorescence. The data are presented as mean ± SD, $n = 3$, $^{*}p < 0.05$, $^{**}p < 0.01$, $^{***}p < 0.001$, *indicates the p-value in comparison to HSA; $^{\#}p < 0.05$, $^{\#\#}p < 0.01$, $^{\#\#\#}p < 0.001$, $^{\#}$indicates the p-value in comparison to G.HSA.

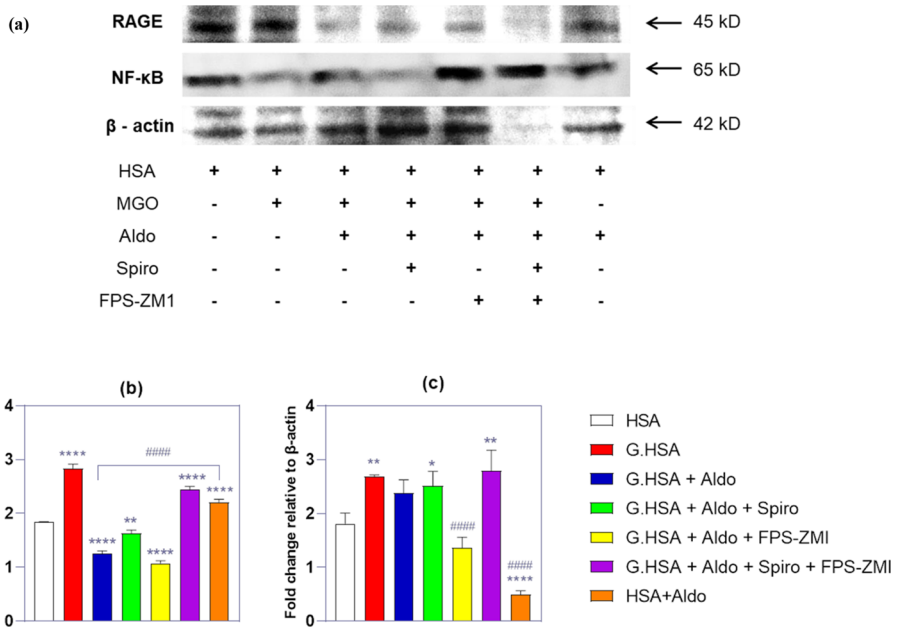

Figure 3. G.HSA + Aldo effect on RAGE and NF-κB protein expressions in renal cells. HEK293T cells, after 24 h treatment of glycated samples (200 μg/mL), were lysed and lysates were used for Western blotting - (a) RAGE, NF-κB and β-actin expressions in cells treated with glycated HSA samples; ratio of (b) RAGE and (c) NF-κB to β-actin by densitometry analysis. The data are presented as mean ± SD, $n = 3$, $^{*}p < 0.05$, $^{**}p < 0.01$, $^{***}p < 0.001$, $^{****}p < 0.0001$, *indicates p value in comparison to HSA; $^{\#}p < 0.05$, $^{\#\#}p < 0.01$, $^{\#\#\#}p < 0.001$, $^{\#\#\#\#}p < 0.0001$, $^{\#}$indicates the p-value in comparison to G.HSA.

increased NF-κB expression ($p < 0.05$); however, spironolactone had no effect. FPS-ZM1 action lowered NF-κB protein levels considerably ($p < 0.0001$) (Figure 3c). This indicates that NF-κB activation is solely RAGE-dependent.

3.4. Aldo Effect on the Gene Expressions of RAGE, NF-κB, MR, and Rac-1. The exposure of G.HSA + Aldo raised gene expression of RAGE ($p < 0.0001$) (Figure 4) compared to that of G.HSA and HSA + Aldo, suggesting the role of Aldo in AGEs accumulation and further interaction with RAGE. Spironolactone did not show any effect on RAGE expression. Conversely, FPS-ZM1 increased RAGE expression compared to G.HSA (Figure 4a). NF-κB expression was also elevated ($p < 0.0001$) (Figure 4b) with the treatment of G.HSA + Aldo. G.HSA and G.HSA + Aldo presence amplified expression of MR ($p < 0.0001$) (Figure 4c) as compared to the treatments of HSA and HSA + Aldo, indicating the role of AGEs in MR activation. Rac-1 expression (Figure 4d) was augmented ($p < 0.1$) in the presence of G.HSA + Aldo, although it was not affected by the presence of

https://doi.org/10.1021/acsomega.3c05085
ACS Omega 2023, 8, 37264−37273

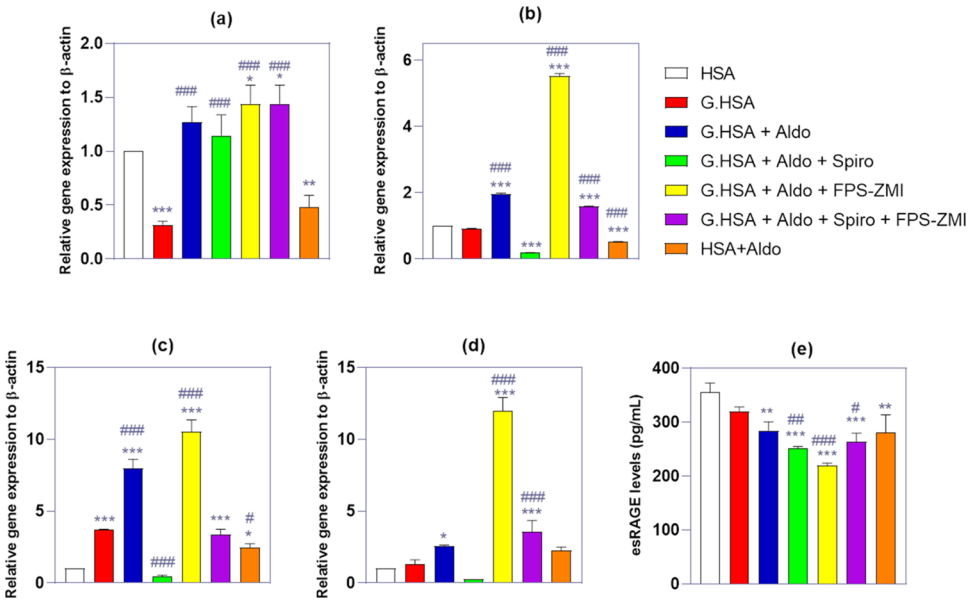

Figure 4. G.HSA + Aldo increases mRNA levels after treatment in renal cells. The treatment of glycated samples was given to HEK293T cells for 24 h and further isolation of mRNA was followed by cDNA synthesis to analyze gene expressions of − (a) RAGE; (b) NF-κB; (c) MR; (d) Rac-1, and (e) esRAGE concentration in cell lysates. The data are presented as mean ± SD, $n = 3$, $^{*}p < 0.05$, $^{**}p < 0.01$, $^{***}p < 0.001$, *indicates p value in comparison to HSA; $^{\#}p < 0.05$, $^{\#\#}p < 0.01$, $^{\#\#\#}p < 0.001$, $^{\#}$indicates p value in comparison to G.HSA.

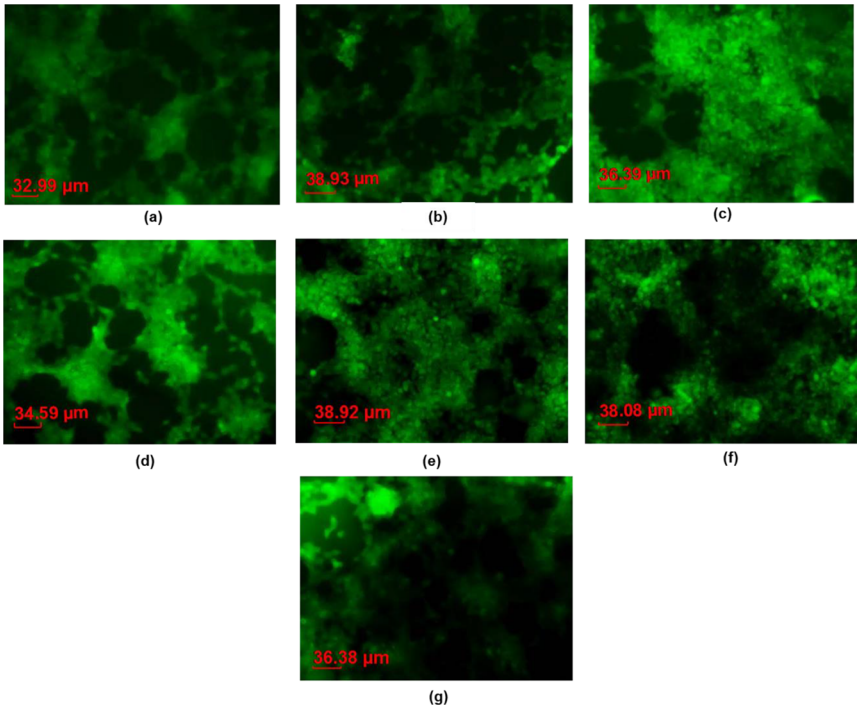

Figure 5. Intracellular ROS generation in response to treatment of glycated HSA and Aldo − (a) Control; (b) HSA; (c) G.HSA; (d) G.HSA + Aldo; (e) G.HSA + Aldo + Spiro; (f) G.HSA + Aldo + FPS-ZM1; (g) G.HSA + Aldo + Spiro + FPS-ZM1.

G.HSA. Spironolactone action reduced the expressions of MR and Rac-1, and FPS-ZM1 maximized NF-κB, MR, and Rac-1 expressions. However, the presence of both antagonists (FPS-ZM1 and spironolactone) reduced expressions of the same three.

esRAGE levels in G.HSA + Aldo were lower ($p < 0.01$) as compared to the treatment given with HSA and G.HSA; however, with the antagonists (FPS-ZM1 and spironolactone), esRAGE levels decreased more significantly ($p < 0.1$) compared to G.HSA (Figure 4e).

3.5. Effect of Aldo on Intracellular Oxidative Stress.

The downstream signaling pathways of the RAGE and MR generate oxidative stress. The estimation of intracellular oxidative stress was carried out by using DCF-DA fluorescence. The fluorescence increased with the treatment of G.HSA as compared to control and treatment with native HSA. However, less fluorescence was observed in G.HSA + Aldo compared to

https://doi.org/10.1021/acsomega.3c05085
ACS Omega 2023, 8, 37264−37273

G.HSA. In the presence of spironolactone or FPS-ZM1 or both, low fluorescence was observed, indicating reduced ROS generation (Figure 5).

4. DISCUSSION

AGEs interaction with RAGE has an essential physiological role in the development of DN.[24] In addition, increased Aldo secretion and upregulation of MR lead to inflammation and renal damage.[25] Both of these signaling cascades are known to activate Rac-1 independently.[6,10] Nonetheless, the crosstalk between AGEs-RAGE and Aldo-MR pathways is yet to be understood. The current study highlights the influence of Aldo on albumin glycation and its interaction with the AGEs-RAGE pathway through Rac-1.

Accumulation of MGO in plasma is often considered a urinary marker for diabetic nephropathy.[26] MGO is a highly reactive compound and a potent glycating agent. Despite its lower physiological concentration than glucose, it is still reported to be 20,000-fold more reactive than glucose.[7,27]

Fructosamine, an early Amadori product of glycation, is used to measure long-term glycemic control.[28] Furthermore, these Amadori products after undergoing rearrangements and complex condensation reactions generate glycation adducts such as protein carbonyls and protein aggregates.[7] These protein carbonyls, with further rearrangements, generate fluorescent and nonfluorescent AGEs.[29] The impact of Aldo on glycation at different stages was evaluated for the first time in this study. The fructosamine content, AGEs, and pentosidine fluorescence in G.HSA + Aldo samples were identical to those observed in the G.HSA treatment. Moreover, phytosterols are reported to reduce Trp-intensity in a dose-dependent manner.[21] The intensity of tryptophan fluorescence of albumin is inversely proportional to steroid concentration, indicating the interaction of steroids with HSA.[30] Our recent study showed that Aldo binds to HSA with high affinity which is static and spontaneous.[15] Pharmacology relevant range of aminoguanidine concentration is reported to be 10−50 μM.[31] In the present study, 100 nM concentration of Aldo is used.[17] However, to understand the mode of action of Aldo 100 nM aminoguanidine was used as a standard inhibitor. Since 100 nM concentration of aminoguanidine is not enough to inhibit glycation, we observed no effect of aminoguanidine on fructosamine content and AGEs fluorescence. We also observed no significant effect of aminoguanidine in our previous study.[15]

RAGE, a multiligand receptor, belongs to the immunoglobulin superfamily.[7] Its expression is significantly upregulated by the G.HSA treatment as also reported by others,[32] which further induces inflammation. The AGEs-RAGE interaction activates multiple cellular kinase pathways and translocates activated NF-κB to the nucleus, further upregulating expressions of pro-inflammatory cytokines.[33] The circulating esRAGE, one of the isoforms of RAGE, may have an essential role in ligand-RAGE-induced inflammation,[34] and it has been associated with severe renal dysfunction in patients of type 2 diabetes.[35] In this study, we found that G.HSA and G.HSA + Aldo decreased the levels of esRAGE.

Moreover, diabetes-induced chronic kidney failure is associated with increased secretion of Aldo which promotes fibrosis, inflammation, and hypertension further reducing the glomerular filtration rate.[36] Aldo-MR activation is reported to be a critical factor in the early pathogenesis of renal damage in diabetes mellitus.[37] It was reported that Aldo stimulates MR activity and regulates gene expression via a genomic pathway.[38] Aldo also stimulates MR-dependent and MR-independent molecular pathways via a nongenomic phenomenon which includes ROS generation and activation of protein kinase A and C, MAPK, and Rac-1.[4]

The present study reported that G.HSA + Aldo induced upregulation of RAGE and NF-κB, whereas G.HSA elevated MR expression compared to HSA + Aldo. This suggests the significant role of AGEs-Aldo in activating the RAGE and MR pathway. Few studies indicated the cellular and molecular crosstalk between Aldo and RAGE. Aldo's presence increased RAGE expression in a positive feedback loop in murine podocyte cells and AGEs-RAGE interaction was also found to upregulate MR expression.[2] In this study, elevated RAGE expression in human renal cells indicates the role of Aldo in glycation via the AGEs-RAGE pathway. However, this interaction can be MR-dependent since spironolactone reduced RAGE protein levels.

Rac-1, from the GTPases family, regulates multiple cellular functions such as ROS generation, actin cytoskeleton organization, cell adhesion, migration, and apoptosis.[39] Overall, its activation contributes to oxidative stress, hypertension, and podocyte injury involved in DN progression.[40] Rac-1-induced oxidative stress is known to regulate and activate NF-κB.[6,39] Increased ROS generation is observed in the presence of G.HSA and G.HSA + Aldo. Additionally, it was reported that MR stimulated Rac-1 activation and ROS generation to produce more AGEs.[2] The data represented by Shibata et al.,[5] reported Rac-1-dependent MR transcriptional activity in the genomic pathway in renal cells. It was found that MR antagonism or MR gene knockout in muscle cells limited the Rac-1-mediated MR signaling.[41] Additionally, AGEs accumulation phosphorylates NF-κB and further upregulates proinflammatory cytokines via activation of Rac-1.[6] In this study, we reported that G.HSA + Aldo upregulates Rac-1 expression.

Considering the involvement of Aldo in inflammation by stimulating NF-κB, it is clinically managed by antagonists. The use of one of the known Aldo inhibitors−spironolactone is shown to reduce NF-κB expression and inflammatory cytokines and reduce blood glucose levels in the type 2 diabetes model mice.[42,43] Also, with the crucial role of RAGE in inflammation, it is targeted for the development of promising treatment modalities. RAGE antagonist, FPS-ZM1, blocked the increased levels of RAGE and down-regulated NF-κB activation,[44] thereby reducing podocyte injury, renal tubular epithelial damage, and urinary albumin excretion in diabetic mice.[11] Indirect studies have indicated the relationship between Aldo and glycation. It was demonstrated that AGEs-induced RAGE expression and NF-κB activation were entirely blocked by MR antagonist spironolactone,[45] disrupting its associated inflammatory cascades.[14] In this study, neither spironolactone showed any effect on RAGE expression nor FPS-ZM1 had its impact on MR. However, both were effective in reducing glycation modifications, independently. Rather than FPS-ZM1, spironolactone reduced Rac-1 and NF-κB expressions, indicating MR-dependent activation of Rac-1 and NF-κB. However, the combination of both antagonists did reduce expressions of RAGE, MR, Rac-1, and NF-κB.

The overall data show that the AGEs + Aldo-RAGE interaction upregulates the MR expression (RAGE-dependent pathway) and AGEs + Aldo upregulates RAGE via the MR-independent pathway, correlating RAGE and MR pathways. It is noteworthy to see the elevated levels of MR when AGEs + Aldo and FPS-ZM1 (RAGE antagonist) exist together, suggesting the

https://doi.org/10.1021/acsomega.3c05085
ACS Omega 2023, 8, 37264−37273

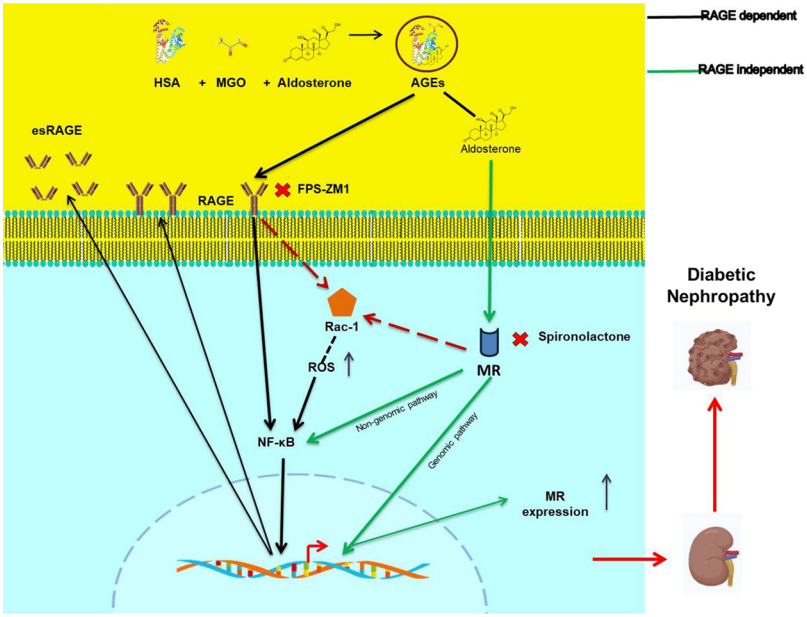

Figure 6. Schematic representation of AGEs-RAGE and Aldo-MR pathway interaction through Rac-1 leading to renal damage. Initially albumin glycation increases in the presence of aldosterone. Further treatment G.HSA + Aldo to cells leads to the NF- κB translocation through RAGE dependent and independent pathway. Activated MR influences NF- κB translocation either by genomic and nongenomic routes. Spironolactone and FPS-ZM1 inhibited MR and RAGE cellular signaling, respectively. Additionally, esRAGE generation increases through this interaction. Overall, this cross talk results in increased gene expression of MR, NF- κB, and RAGE leading to DN.

involvement of other AGE receptors (RAGE-independent pathway). The AGEs + Aldo-MR pathway activates Rac-1 and NF-κB, indicating the coreliability of AGEs and Aldo to cause further renal damage via Rac-1. The decreased glycation modifications and reduced expression of RAGE, MR, Rac-1, and NF-κB in the presence of spironolactone and FPS-ZM1 suggested interaction between two pathways.

5. CONCLUSIONS

The present study revealed the role of Aldo and enhanced glycation in DN. The combination of spironolactone and FPS-ZM1 discovered the molecular crosstalk between AGEs-RAGE and Aldo-MR through Rac-1 (Figure 6). The combined action of both antagonists carries a therapeutic value in treating DN. Furthermore, activation of the RAGE-independent pathway may generate oxidative stress and inflammation, thus deteriorating renal damage. Hence, the study of AGEs-RAGE and Aldo-MR pathways with the help of pharmacological interventions may suppress RAGE-dependent and -independent pathways efficiently. In the future, this specific treatment strategy will be more beneficial to alleviate DN and its associated complications.

■ ASSOCIATED CONTENT

Supporting Information

The Supporting Information is available free of charge at https://pubs.acs.org/doi/10.1021/acsomega.3c05085.

Cellular morphology at 0 and 24 h after treatment with G.HSA and Aldo at 40 X; cell viability after treatment of G.HSA and Aldo (PDF)

■ AUTHOR INFORMATION

Corresponding Author

Rashmi S. Tupe − *Symbiosis School of Biological Sciences, Symbiosis International (Deemed University) (SIU), Pune, Maharashtra State 412115, India;* orcid.org/0000-0002-6726-3601; Phone: +91 9922263074; Email: rashmi.tupe@ssbs.edu.in

Authors

Mayura Apte − *Symbiosis School of Biological Sciences, Symbiosis International (Deemed University) (SIU), Pune, Maharashtra State 412115, India*

Mohd Shahnawaz Khan − *Department of Biochemistry, College of Science, King Saud University, Riyadh 11451, Saudi Arabia*

Nilima Bangar − *Symbiosis School of Biological Sciences, Symbiosis International (Deemed University) (SIU), Pune, Maharashtra State 412115, India*

Armaan Gvalani − *Symbiosis School of Biological Sciences, Symbiosis International (Deemed University) (SIU), Pune, Maharashtra State 412115, India*

Huma Naz − *Department of Internal Medicine, University of Missouri, Columbia, Missouri 65211, United States*

Complete contact information is available at: https://pubs.acs.org/10.1021/acsomega.3c05085

Author Contributions

All authors contributed to the study conception and design. Material preparation, data collection, and analysis were performed by M.A. The first draft of the manuscript was written by M.A. and all authors commented on previous versions of the manuscript. All authors read and approved the final manuscript.

Funding

The authors declare that no funds, grants, or other support were received during the preparation of this manuscript.

Notes

This article does not contain any studies with human participants or animals performed by any of the authors.

The authors declare no competing financial interest.

■ ACKNOWLEDGMENTS

M.S.K. acknowledges the generous support from the Research Supporting Project (RSP2023R352) by the King Saud University, Riyadh, Kingdom of Saudi Arabia. We greatly acknowledge the support provided by Dr. Selvan Ravindran, SSBS, SIU, for the HPLC analysis of the research study.

■ ABBREVIATIONS

AG: aminoguanidine
AGEs: advanced glycation end products
Aldo: aldosterone
CML: carboxymethyl lysine
DN: diabetic nephropathy
esRAGE: endogenously secretory RAGE
FL-RAGE: full length RAGE
FPS-ZMI: N-benzyl-4-chloro-N-cyclohexylbenzamide.
HEK293T: human embryonic kidney cells transfected with SV40 T-antigen
HSA: human serum albumin
MGO: methylglyoxal
MR: mineralocorticoid receptor
NF-κB: nuclear factor κ-B
Rac1: Ras-related C3 botulinum toxin substrate
RAGE: receptor of advanced glycation end products
RAS: renin angiotensin system
ROS: reactive oxygen species

■ REFERENCES

(1) Goh, S. Y.; Cooper, M. E. The Role of Advanced Glycation End Products in Progression and Complications of Diabetes. *J. Clin. Endocrinol. Metab.* **2008**, *93* (4), 1143−1152.
(2) Taguchi, K.; Yamagishi, S. I.; Yokoro, M.; Ito, S.; Kodama, G.; Kaida, Y.; Nakayama, Y.; Ando, R.; Yamada-Obara, N.; Asanuma, K.; Matsui, T.; Higashimoto, Y.; Brooks, C. R.; Ueda, S.; Okuda, S.; Fukami, K. RAGE-Aptamer Attenuates Deoxycorticosterone Acetate/Salt-Induced Renal Injury in Mice. *Sci. Rep.* **2018**, *8* (1), 2686 DOI: 10.1038/s41598-018-21176-5.
(3) Cannavo, A.; Bencivenga, L.; Liccardo, D.; Elia, A.; Marzano, F.; Gambino, G.; D'Amico, M. L.; Perna, C.; Ferrara, N.; Rengo, G.; Paolocci, N. Aldosterone and Mineralocorticoid Receptor System in Cardiovascular Physiology and Pathophysiology. *Oxid. Med. Cell. Longev.* **2018**, *2018*, No. 1204598.
(4) Mihailidou, A. S. Nongenomic Actions of Aldosterone: Physiological or Pathophysiological Role? *Steroids* **2006**, *71* (4), 277−280.
(5) Shibata, S.; Nagase, M.; Yoshida, S.; Kawarazaki, W.; Kurihara, H.; Tanaka, H.; Miyoshi, J.; Takai, Y.; Fujita, T. Modification of Mineralocorticoid Receptor Function by Rac1 GTPase: Implication in Proteinuric Kidney Disease. *Nat. Med.* **2008**, *14* (12), 1370−1376.
(6) Dong, N.; Xu, B.; Shi, H.; Lu, Y. MiR-124 Regulates Amadori-Glycated Albumin-Induced Retinal Microglial Activation and Inflammation by Targeting Rac1. *Investig. Ophthalmol. Vis. Sci.* **2016**, *57* (6), 2522−2532.
(7) Vetter, S. W. *Glycated Serum Albumin and AGE Receptors*, 1st ed.; Elsevier Inc., 2015; Vol. 72.
(8) Sanajou, D.; Ghorbani Haghjo, A.; Argani, H.; Aslani, S. AGE-RAGE Axis Blockade in Diabetic Nephropathy: Current Status and Future Directions. *Eur. J. Pharmacol.* **2018**, *833*, 158−164.
(9) Walke, P. B.; Bansode, S. B.; More, N. P.; Chaurasiya, A. H.; Joshi, R. S.; Kulkarni, M. J. Molecular Investigation of Glycated Insulin-Induced Insulin Resistance via Insulin Signaling and AGE-RAGE Axis. *Biochim. Biophys. Acta, Mol. Basis Dis.* **2021**, *1867* (2), No. 166029.
(10) Hudson, B. I.; Kalea, A. Z.; Del Mar Arriero, M.; Harja, E.; Boulanger, E.; D'Agati, V.; Schmidt, A. M. Interaction of the RAGE Cytoplasmic Domain with Diaphanous-1 Is Required for Ligand-Stimulated Cellular Migration through Activation of Rac1 and Cdc42. *J. Biol. Chem.* **2008**, *283* (49), 34457−34468.
(11) Sanajou, D.; Ghorbani Haghjo, A.; Argani, H.; Roshangar, L.; Rashtchizadeh, N.; Ahmad, S. N. S.; Ashrafi-Jigheh, Z.; Bahrambeigi, S.; Asiaee, F.; Rashedi, J.; Aslani, S. Reduction of Renal Tubular Injury with a RAGE Inhibitor FPS-ZM1, Valsartan and Their Combination in Streptozotocin-Induced Diabetes in the Rat. *Eur. J. Pharmacol.* **2019**, *842*, 40−48.
(12) Steenbeke, M.; De Bruyne, S.; De Buyzere, M.; Lapauw, B.; Speeckaert, R.; Petrovic, M.; Delanghe, J. R.; Speeckaert, M. M. The Role of Soluble Receptor for Advanced Glycation End-Products (SRAGE) in the General Population and Patients with Diabetes Mellitus with a Focus on Renal Function and Overall Outcome. *Crit. Rev. Clin. Lab. Sci.* **2021**, *58* (2), 113−130, DOI: 10.1080/10408363.2020.1791045.
(13) Scavello, F.; Zeni, F.; Tedesco, C. C.; Mensà, E.; Veglia, F.; Procopio, A. D.; Bonfigli, A. R.; Olivieri, F.; Raucci, A. Modulation of Soluble Receptor for Advanced Glycation End-Products (RAGE) Isoforms and Their Ligands in Healthy Aging. *Aging* **2019**, *11* (6), 1648−1663.
(14) Wang, C. C.; Lee, A. S.; Liu, S. H.; Chang, K. C.; Shen, M. Y.; Chang, C. T. Spironolactone Ameliorates Endothelial Dysfunction through Inhibition of the AGE/RAGE Axis in a Chronic Renal Failure Rat Model. *BMC Nephrol.* **2019**, *20* (1), 351 DOI: 10.1186/s12882-019-1534-4.
(15) Gaikwad, D. D.; Bangar, N. S.; Apte, M. M.; Gvalani, A.; Tupe, R. S. Mineralocorticoid Interaction with Glycated Albumin Down-regulates NRF − 2 Signaling Pathway in Renal Cells: Insights into Diabetic Nephropathy. *Int. J. Biol. Macromol.* **2022**, *220*, 837−851.
(16) Soudahome, A. G.; Catan, A.; Giraud, P.; Kouao, S. A.; Guerin-Dubourg, A.; Debussche, X.; Le Moullec, N.; Bourdon, E.; Bravo, S. B.; Paradela-Dobarro, B.; Álvarez, E.; Meilhac, O.; Rondeau, P.; Couprie, J. Glycation of Human Serum Albumin Impairs Binding to the Glucagon-like Peptide-1 Analogue Liraglutide. *J. Biol. Chem.* **2018**, *293* (13), 4778−4791.
(17) Queisser, N.; Oteiza, P. I.; Link, S.; Hey, V.; Stopper, H.; Schupp, N. Aldosterone Activates Transcription Factor Nrf2 in Kidney Cells Both in Vitro and in Vivo. *Antioxid. Redox Signaling* **2014**, *21* (15), 2126−2142.
(18) Lowry, O. H.; Rosebrough, N. J.; Farr, A. L.; Randall, R. J. Protein Measurement with the Folin Phenol Reagent. *J. Biol. Chem.* **1951**, *193* (1), 265−275.
(19) Baker, J. R.; Metcalf, P. A.; Johnson, R. N.; Newman, D.; Rietz, P. Use of Protein-Based Standards in Automated Colorimetric Determinations of Fructosamine in Serum. *Clin. Chem.* **1985**, *31* (9), 1550−1554.
(20) Uchida, K.; Kanematsu, M.; Sakai, K.; Matsuda, T.; Hattori, N.; Mizuno, Y.; Suzuki, D.; Miyata, T.; Noguchi, N.; Niki, E.; Osawa, T. Protein-Bound Acrolein: Potential Markers for Oxidative Stress. *Proc. Natl. Acad. Sci. U. S. A.* **1998**, *95* (9), 4882−4887.
(21) Sobhy, R.; Khalifa, I.; Liang, H.; Li, B. Phytosterols Disaggregate Bovine Serum Albumin under the Glycation Conditions through Interacting with Its Glycation Sites and Altering Its Secondary Structure Elements. *Bioorg. Chem.* **2020**, *101*, No. 104047.
(22) Adeshara, K. A.; Agrawal, S. B.; Gaikwad, S. M.; Tupe, R. S. Pioglitazone Inhibits Advanced Glycation Induced Protein Modifications and Down-Regulates Expression of RAGE and NF-KB in Renal Cells. *Int. J. Biol. Macromol.* **2018**, *119*, 1154−1163.
(23) Tupe, R. S.; Sankhe, N. M.; Shaikh, S. A.; Phatak, D. V.; Parikh, J. U.; Khaire, A. A.; Kemse, N. G. Aqueous Extract of Some Indigenous Medicinal Plants Inhibits Glycation at Multiple Stages and Protects Erythrocytes from Oxidative Damage−an in Vitro Study. *J. Food Sci. Technol.* **2015**, *52* (4), 1911−1923.
(24) Fukami, K.; Taguchi, K.; Yamagishi, S. I.; Okuda, S. Receptor for Advanced Glycation Endproducts and Progressive Kidney Disease. *Curr. Opin. Nephrol. Hypertens.* **2015**, *24* (1), 54−60.
(25) Funder, J. W. Aldosterone and Mineralocorticoid Receptors—Physiology and Pathophysiology. *Int. J. Mol. Sci.* **2017**, *18* (5), 1032 DOI: 10.3390/ijms18051032.

(26) Pastor-Belda, M.; Fernández-García, A. J.; Campillo, N.; Pérez-Cárceles, M. D.; Motas, M.; Hernández-Córdoba, M.; Viñas, P. Glyoxal and Methylglyoxal as Urinary Markers of Diabetes. Determination Using a Dispersive Liquid−Liquid Microextraction Procedure Combined with Gas Chromatography−Mass Spectrometry. *J. Chromatogr. A* **2017**, *1509*, 43−49.
(27) Schalkwijk, C. G.; Stehouwer, C. D. A. Methylglyoxal, a Highly Reactive Dicarbonyl Compound, in Diabetes, Its Vascular Complications, and Other Age-Related Diseases. *Physiol. Rev.* **2020**, *100* (1), 407−461.
(28) Peer, N.; George, J.; Lombard, C.; Levitt, N.; Kengne, A.-P. Associations of Glycated Albumin and Fructosamine with Glycaemic Status in Urban Black South Africans. *Clin. Chim. Acta* **2021**, *519*, 291−297.
(29) Perrone, A.; Giovino, A.; Benny, J.; Martinelli, F. Advanced Glycation End Products (AGEs): Biochemistry, Signaling, Analytical Methods, and Epigenetic Effects. *Oxid. Med. Cell. Longevity* **2020**, *2020*, No. 3818196.
(30) Wu, Y.; Mitchell, J.; Cook, C.; Main, L. Evaluation of Progesterone-Ovalbumin Conjugates with Different Length Linkers in Enzyme-Linked Immunosorbant Assay and Surface Plasmon Resonance-Based Immunoassay. *Steroids* **2002**, *67* (7), 565−572.
(31) Thornalley, P. J.; Yurek-George, A.; Argirov, O. K. Kinetics and Mechanism of the Reaction of Aminoguanidine with the α-Oxoaldehydes Glyoxal, Methylglyoxal, and 3-Deoxyglucosone under Physiological Conditions. *Biochem. Pharmacol.* **2000**, *60* (1), 55−65.
(32) Hudson, B. I.; Lippman, M. E. Targeting RAGE Signaling in Inflammatory Disease. *Annu. Rev. Med.* **2018**, *69*, 349−364, DOI: 10.1146/annurev-med-041316-085215.
(33) An, X.; Zhang, L.; Yao, Q.; Li, L.; Wang, B.; Zhang, J.; He, M.; Zhang, J. The Receptor for Advanced Glycation Endproducts Mediates Podocyte Heparanase Expression through NF-KB Signaling Pathway. *Mol. Cell. Endocrinol.* **2018**, *470*, 14−25.
(34) Choi, K. M.; Yoo, H. J.; Kim, H. Y.; Lee, K. W.; Seo, J. A.; Kim, S. G.; Kim, N. H.; Choi, D. S.; Baik, S. H. Association between Endogenous Secretory RAGE, Inflammatory Markers and Arterial Stiffness. *Int. J. Cardiol.* **2009**, *132* (1), 96−101.
(35) Gohda, T.; Tanimoto, M.; Moon, J. Y.; Gotoh, H.; Aoki, T.; Matsumoto, M.; Shibata, T.; Ohsawa, I.; Funabiki, K.; Tomino, Y. Increased Serum Endogenous Secretory Receptor for Advanced Glycation End-Product (EsRAGE) Levels in Type 2 Diabetic Patients with Decreased Renal Function. *Diabetes Res. Clin. Pract.* **2008**, *81* (2), 196−201.
(36) Tesch, G. H.; Young, M. J. Mineralocorticoid Receptor Signaling as a Therapeutic Target for Renal and Cardiac Fibrosis. *Front. Pharmacol.* **2017**, *8*, 313 DOI: 10.3389/fphar.2017.00313.
(37) Guo, C.; Martinez-Vasquez, D.; Mendez, G. P.; Toniolo, M. F.; Yao, T. M.; Oestreicher, E. M.; Kikuchi, T.; Lapointe, N.; Pojoga, L.; Williams, G. H.; Ricchiuti, V.; Adler, G. K. Mineralocorticoid Receptor Antagonist Reduces Renal Injury in Rodent Models of Types 1 and 2 Diabetes Mellitus. *Endocrinology* **2006**, *147* (11), 5363−5373.
(38) Ong, G. S. Y.; Young, M. J. Mineralocorticoid Regulation of Cell Function: The Role of Rapid Signalling and Gene Transcription Pathways. *J. Mol. Endocrinol.* **2017**, *58* (1), R33−R57.
(39) Tong, L.; Tergaonkar, V. Rho Protein GTPases and Their Interactions with NF?B: Crossroads of Inflammation and Matrix Biology. *Biosci. Rep.* **2014**, *34* (3), No. e00115, DOI: 10.1042/BSR20140021.
(40) Hirohama, D.; Nishimoto, M.; Ayuzawa, N.; Kawarazaki, W.; Fujii, W.; Oba, S.; Shibata, S.; Marumo, T.; Fujita, T. Activation of Rac1-mineralocorticoid Receptor Pathway Contributes to Renal Injury in Salt-Loaded Db/Db Mice. *Hypertension* **2021**, *78* (1), 82−93.
(41) Barrera-Chimal, J.; André-Grégoire, G.; Cat, A. N. D.; Lechner, S. M.; Cau, J.; Prince, S.; Kolkhof, P.; Loirand, G.; Sauzeau, V.; Hauet, T.; Jaisser, F. Benefit of Mineralocorticoid Receptor Antagonism in AKI: Role of Vascular Smooth Muscle Rac1. *J. Am. Soc. Nephrol.* **2017**, *28* (4), 1216−1226.
(42) Ferreira, N. S.; Bruder-Nascimento, T.; Pereira, C. A.; Zanotto, C. Z.; Prado, D. S.; Silva, J. F.; Rassi, D. M.; Foss-Freitas, M. C.; Alves-Filho, J. C.; Carlos, D.; de Cássia Tostes, R. NLRP3 Inflammasome and Mineralocorticoid Receptors Are Associated with Vascular Dysfunction in Type 2 Diabetes Mellitus. *Cells* **2019**, *8* (12), 1595 DOI: 10.3390/cells8121595.
(43) Sønder, S. U. S.; Woetmann, A.; Ødum, N.; Bendtzen, K. Spironolactone Induces Apoptosis and Inhibits NF-KB Independent of the Mineralocorticoid Receptor. *Apoptosis* **2006**, *11* (12), 2159−2165.
(44) Shen, L.; Zhang, T.; Yang, Y.; Lu, D.; Xu, A.; Li, K. FPS-ZM1 Alleviates Neuroinflammation in Focal Cerebral Ischemia Rats via Blocking Ligand/RAGE/DIAPH1 Pathway. *ACS Chem. Neurosci.* **2021**, *12* (1), 63−78.
(45) Matsui, T.; Takeuchi, M.; Yamagishi, S. Ichi. Nifedipine, a Calcium Channel Blocker, Inhibits Inflammatory and Fibrogenic Gene Expressions in Advanced Glycation End Product (AGE)-Exposed Fibroblasts via Mineralocorticoid Receptor Antagonistic Activity. *Biochem. Biophys. Res. Commun.* **2010**, *396* (2), 566−570.
(46) Yao, D.; Brownlee, M. Hyperglycemia-Induced Reactive Oxygen Species Increase Expression of the Receptor for Advanced Glycation End Products (RAGE) and RAGE Ligands. *Diabetes* **2010**, *59* (1), 249−255.
(47) Syed, A. A.; Reza, M. I.; Shafiq, M.; Kumariya, S.; Singh, P.; Husain, A.; Hanif, K.; Gayen, J. R. Naringin Ameliorates Type 2 Diabetes Mellitus-Induced Steatohepatitis by Inhibiting RAGE/NF-KB Mediated Mitochondrial Apoptosis. *Life Sci.* **2020**, *257*, No. 118118.
(48) Yang, J.; Fuller, P. J.; Morgan, J.; Shibata, H.; Clyne, C. D.; Young, M. J. GEMIN4 Functions as a Coregulator of the Mineralocorticoid Receptor. *J. Mol. Endocrinol.* **2015**, *54* (2), 149−160.
(49) Tian, F.; Wang, Z.; He, J.; Zhang, Z.; Tan, N. 4-Octyl Itaconate Protects against Renal Fibrosis via Inhibiting TGF-β/Smad Pathway, Autophagy and Reducing Generation of Reactive Oxygen Species. *Eur. J. Pharmacol.* **2020**, *873*, No. 172989.
(50) Chuong, C.; Katz, J.; Pauley, K. M.; Bulosan, M.; Cha, S. RAGE Expression and NF-KappaB Activation Attenuated by Extracellular Domain of RAGE in Human Salivary Gland Cell Line. *J. Cell. Physiol.* **2009**, *221* (2), 430−434.

https://doi.org/10.1021/acsomega.3c05085
ACS Omega 2023, 8, 37264−37273